Photooxidation of cyclohexene in the presence of SO$_2$: SOA yield and chemical composition

Shijie Liu[1,2,3], Long Jia[2], Yongfu Xu[2], Narcisse T. Tsona[1], Shuangshuang Ge[2], Lin Du[3,1,2]

[1]Environment Research Institute, Shandong University, Jinan, 250100, China
5 [2]State Key Laboratory of Atmospheric Boundary Layer Physics and Atmospheric Chemistry, Institute of Atmospheric Physics, Chinese Academy of Sciences, Beijing, 100029, China
[3]Shenzhen Research Institute, Shandong University, Shenzhen, 518057, China

Correspondence to: Lin Du (lindu@sdu.edu.cn); Yongfu Xu (xyf@mail.iap.ac.cn)

Abstract. Secondary organic aerosol (SOA) formation from cyclohexene/NOx system with various SO$_2$ concentrations
10 under UV light was investigated to study the effects of cyclic alkenes on the atmospheric environment in polluted urban areas. A clear decrease at first and then increase of the SOA yield was found with increasing SO$_2$ concentrations. The lowest SOA yield was obtained when initial SO$_2$ concentration was in the range of 30-40 ppb, while higher SOA yield compared to that without SO$_2$ could not be obtained until the initial SO$_2$ concentration was higher than 85 ppb. The decreasing SOA yield might be due to the fact that the promoting effect of acid-catalyzed reactions on SOA formation was less important than the
15 inhibiting effect of decreasing OH concentration at low initial SO$_2$ concentrations, caused by the competition reactions of OH with SO$_2$ and cyclohexene. The competitive reaction was an important factor for SOA yield and it should not be neglected in photooxidation reactions. The composition of organic compounds in SOA was measured using several complementary techniques including Fourier transform infrared (FTIR) spectrometer, ion chromatograph (IC) and electrospray ionization high-resolution quadrupole mass spectrometer (ESI-HR-MS). We present the first evidence that
20 organosulfates were produced from the photooxidation of cyclohexene in the presence of SO$_2$.

1 Introduction

Alkenes are widely emitted from biogenic and anthropogenic sources (Kesselmeier et al., 2002; Chin and Batterman, 2012), and their gas-phase oxidation reactions with OH, NO$_3$, or O$_3$ are among the most important processes in the atmosphere (Atkinson, 1997; Stewart et al., 2013; Paulson et al., 1999). The reactions of ozone with alkenes are an important source of
25 free radicals in the lower atmosphere, which influence the oxidative capacity of the atmosphere (Paulson and Orlando, 1996). Some of the products have sufficiently low vapor pressures to condense with other gaseous species, and contribute to the secondary organic aerosol (SOA) mass (Sarwar and Corsi, 2007; Sakamoto et al., 2013; Nah et al., 2016; Kroll and Seinfeld, 2008; Hallquist et al., 2009). SOA formation from VOCs oxidation has been receiving significant attention since recent years due to its large implication in the formation of atmospheric fine particulate matter (Jimenez et al., 2009). SOA has significant

impacts on human health (Pope III and Dockery, 2006), air quality (Kanakidou et al., 2005; Jaoui et al., 2012; McFiggans et al., 2006), and global climate change (Hansen and Sato, 2001; Adams et al., 2001; Pokhrel et al., 2016).

Although cyclic alkenes widely exist in the atmosphere, their gas-phase oxidation has received less attention than that of linear or branched alkenes (Sipilä et al., 2013). Cyclohexene is an important industrial chemical (Sun et al., 2013), and is also widespread in urban areas (Grosjean et al., 1978). Cyclohexene has been extensively studied as a monoterpene surrogate for inferring oxidation mechanisms and aerosol formation characteristics, because it has the basic structural unit in abundant biogenic monoterpenes and sesquiterpenes (Carlsson et al., 2012; Keywood et al., 2004). The rate constants for gas-phase reactions of cyclohexene with OH, O_3 and NO_3 were measured at room temperature to be $(6.4\pm0.1)\times10^{-11}$, $(8.1\pm1.8)\times10^{-17}$ and $(5.4\pm0.2)\times10^{-13}$ cm^3 molecule^{-1} s^{-1}, respectively (Stewart et al., 2013; Aschmann et al., 2012), and a correlation between the logarithm of the rate constants and the molecular orbital energies for simple cyclic alkenes was observed. The effect of pressure and that of the presence of SO_2 on the formation of stable gas-phase products and SOA from ozonolysis of cyclohexene were investigated (Carlsson et al., 2012). It was found that the collisional stabilization of initial clusters was an important aspect for SOA formation processes involving sulfuric acid (H_2SO_4) and organic compounds. The effect of the structure of the hydrocarbon parent molecule on SOA formation was investigated for a series of cyclic alkenes and related compounds (Keywood et al., 2004), and the SOA yield was found to be a function of the number of carbons present in the cyclic alkenes ring. The relative SOA yields from ozonolysis of cyclic alkenes can be quantitatively predicted from properties of the parent hydrocarbons, like the presence of a methyl group and an exocyclic double bond.

SO_2, one of the most important inorganic pollutants in urban area, plays an important role on SOA formation (Wang et al., 2005; Lonsdale et al., 2012; Liu et al., 2016). Seasonal variations of SO_2 concentrations were found to be consistent with seasonal variations of $PM_{2.5}$ concentration (Cheng et al., 2015). Smog chamber simulations have indicated that SO_2 could enhance the formation of SOA from VOCs oxidation under acidic conditions by increasing aerosol acidity and ammonium sulfate aerosol formation (Edney et al., 2005; Liu et al., 2016; Attwood et al., 2014). Anthropogenic SO_2 emissions can impact new particle formation, and SOA composition (Lonsdale et al., 2012).

Despite the existence of organosulfates in ambient aerosols was first observed in 2005 (Romero and Oehme, 2005), proper identification of these aerosols was made two years later. In a series of chamber experiments studies, it was shown that organosulfates present in ambient aerosols collected from various locations mostly originate from acid-catalyzed reactions of SOA formed from photooxidation of α-pinene and isoprene (Surratt et al., 2007). Recently, different kinds of organosulfates have been observed in SOA around the world, and organosulfates have been identified as a group of compounds that have an important contribution to the total amount of SOA in the atmosphere (Surratt et al., 2008; Froyd et al., 2010; Kristensen and Glasius, 2011; Tolocka and Turpin, 2012; Wang et al., 2015). Laboratory chamber studies showed that OH/NOx/O_3-initiated reactions of BVOCs, such as isoprene, α-pinene, β-pinene, and limonene with sulfates or sulfuric acid are the main processes for organosulfates formation (Surratt et al., 2007; Surratt et al., 2008; Hatch et al., 2011). Despite the well-recognized presence of organosulfates in SOA, their formation and transformation processes can be complex and varied, depending on the nature of the original organic compound involved. Extensive studies on their formation have been performed and several

mechanisms based on a variety of reactions have been proposed. Using nuclear resonance techniques, isoprene-derived epoxides formed during isoprene photooxidation reactions were found to be important intermediates for organonitrates and organosulfates formation via potential SOA reactions (Darer et al., 2011; Hu et al., 2011). The authors further found that organonitrates could easily be transformed to organosulfates during hydrolysis in the presence of sulfate. Some studies also showed that 2-methyl-3-buten-2-ol (MBO), due to its larger emissions than isoprene in some regions (Baker et al., 1999), is an important precursor for organosulfates and SOA in the atmosphere, through its reactions with OH under NO and aerosol acidity conditions, and from acid-catalyzed reactive uptake of MBO-based epoxides formed during MBO photooxidation (Mael et al., 2015; Zhang et al., 2012; Zhang et al., 2014). Organosulfates formation was also found from oxidation of hydroxyhydroperoxides (Riva et al., 2016) and from heterogeneous reactions of SO_2 with selected long-chain alkenes and unsaturated fatty acids (Passananti et al., 2016).

Reactions with sulfates or H_2SO_4 were the main formation processes of organosulfates. Qualitative analyses of the organosulfates in SOA have been gaining more attention and development since recent years (Lin et al., 2012; Shalamzari et al., 2013; Staudt et al., 2014). Riva et al. investigated the formation of organosulfates from photooxidation of polycyclic aromatic hydrocarbons and found that, in the presence of sulfate aerosol, this photooxidation was a hitherto unrecognized source of anthropogenic secondary organosulfur compounds (Riva et al., 2015). A more complete structural characterization of polar organosulfates that originate from isoprene SOA was performed (Shalamzari et al., 2013), and an organosulfate related to methyl vinyl ketone and minor polar organosulfates related to croton aldehyde were identified. However, there was no report about the yield and chemical composition of SOA obtained from photooxidation of cyclohexene in the presence of SO_2.

In the present work, we investigated the SOA yields and chemical composition during cyclohexene photooxidation under different SO_2 concentrations conditions. A better understanding of the magnitude and chemical composition of SOA from different SO_2 concentrations will contribute to more accurate SOA prediction from anthropogenic sources and give valuable information related to air pollution in urban environments.

2 Methods

2.1 Chamber description

The experiments were performed in a 400 L Teflon FEP film chamber (wall thickness 125 μm) at the Institute of Atmospheric Physics, Chinese Academy of Sciences, Beijing. The details of the chamber, including the experimental setup and analysis techniques have been described elsewhere (Du et al., 2007; Jia and Xu, 2014), and only a brief description is presented here. The reactor was surrounded by 12 black light lamps (GE F40BLB) with emission band centered at 365 nm, which were used to simulate the spectrum of the UV band in solar irradiation. Stainless steel was covered on the chamber interior walls to maximize and homogenize the interior light intensity. The effective light intensity near the ultraviolet region plays a decisive role in the formation of photochemical smog (Presto et al., 2005a). The effective light intensity of the

chamber was represented by the photolysis rate constant of NO_2. In our study, the average effective light intensity was determined to be 0.177 min^{-1}. Both inlet and outlet of the chamber were made of Teflon material. Atmospheric pressure was maintained in the chamber at all times. All the experiments were performed at room temperature (307±2 K) under dry conditions (RH < 10%). The wall loss is the decrease of the concentration of reactive gas phase species caused by adsorption on the inner wall of the reactor. Residual reactant and product on the inner wall can also react with the gas phase species, which is another important reason for wall loss. The wall loss can directly affect the quantitative evaluation of the photooxidation rate and SOA yield. A correct estimation of the wall loss is therefore necessary in a reliable analysis of the experimental results of SOA yield. In the present study, the wall loss of cyclohexene in the chamber could be neglected since no decrease in its concentration was observed. The wall loss of O_3, NOx, and SO_2 were first order because $\ln([X]_0/[X]_t)$ had a good correlation with time (R^2=0.994, 0.944, 0.999 for O_3, NOx, and SO_2, respectively). The measured wall loss rate constants for O_3, NOx and SO_2 were 5.05×10⁻⁶, 7.04×10⁻⁶ and 6.39×10⁻⁶ s^{-1}, respectively. The average value of the wall loss rate constant of particles was 4.7×10⁻⁵ s^{-1}, and the measured particle concentrations in this study were corrected using the same method as Pathak et al. (Pathak et al., 2007). Typical profiles of the gas and particle phases are given in Figure S1 of the Supplementary material.

Prior to each experiment, the chamber was cleaned by purging with purified dry air for at least 8 h until residual hydrocarbons, O_3, NOx or particles could not be detected in the reactor. Known amounts of cyclohexene was injected into a 0.635 cm diameter Teflon FEP tube and dispensed into the chamber by purified dry air. Typical initial cyclohexene concentrations were 500 ppb. NOx was injected by a gas-tight syringe to make the mixing ratio of NOx in the reactor around 95 ppb during all the experiments. The mixed concentration ratios of cyclohexene/NOx were in the range 4.4-6.9. SOA formation experiments were carried out under UV irradiation in the presence of NOx to produce O_3 and OH radicals for cyclohexene oxidation. Although initial VOCs, NOx and average OH concentrations were different from typical urban conditions, efforts were made to maintain the initial concentrations of the reactants as similar as possible to make sure the effect of SO_2 was the main reason for the changes in the SOA yield. More details on the experimental conditions are shown in Table 1.

2.2 Gas and particle measurements

Ozone concentration in the reactor was measured using ozone analyzer (Model 49C, Thermo Electron Corporation, USA). A NO-NO_2-NOx analyzer (Model 42C, Thermo Electron Corporation, USA) was used to monitor the NOx concentration. Measurement of SO_2 concentration was made using a SO_2 analyzer (Model 43i-TLE, Thermo Electron Corporation, USA). The uncertainty of the O_3, NOx and SO_2 measurement was less than ±1%. The detection limits of the different monitors were 0.40 ppb, 0.50 ppb, and 0.05 ppb for NOx, O_3, and SO_2, respectively.
Two Tenax absorption tubes (150 mm length × 6 mm O.D., 0.2 g sorbent) were used to collect the sample before the UV lights were turned on and at the end of each experiment, respectively. The volume of the sample was 60 mL and the sampling time was 3 min. The concentrations of cyclohexene were analyzed by thermal desorption-gas chromatography-

mass spectrometry (TD-GC-MS). A thermal desorption unit (Master TD, Dani, Italy) was combined with a 6890A gas chromatograph (6890A, Agilent Tech., USA) interfaced to a 5975C mass selective detector (5975C, Agilent Tech., USA). The GC was equipped with a HP-5MS capillary column (30 m × 0.25 mm, 0.25 μm film thickness). The TD temperature was 280 °C, and the sampling time was 3 min. The GC-MS temperature program was as follows: the initial temperature of 40 °C was held for 4 min, and then raised to 300 °C at a rate of 20 °C min^{-1}. The inlet temperature was set at 250 °C and the transfer line at 200 °C. The ionization method in MS was electron impact ionization, and helium was used as the carrier gas at a constant flow (1.2 mL min^{-1}). Because a very diverse range of compounds might be present in the samples, the SCAN mode (36-500 amu) was used in the MS detector. This mode is known to be a classical and typical detection method for GC-MS analysis. The results were analyzed with MSD Productivity ChemStation.

Particle number concentrations and size distributions were measured with a scanning mobility particle sizer (SMPS), which consists of a differential mobility analyzer (DMA model 3081, TSI Inc., USA) and a condensation particle counter (CPC model 3776, TSI Inc., USA). A sheath flow/aerosol flow relationship of 3.0/0.3 L min^{-1} was used for the measurements. The particle size was measured in the range of 14 to 710 nm, and each scan was 180 s. An aerosol density of 1.2 g cm^{-3} was assumed to convert the particle volume concentration into the mass concentration (Zhang et al., 2015). Size distribution data were recorded and analyzed using the TSI AIM software v9.0.

2.3 Products composition analysis

The chemical composition of SOA was important for analyzing the degree of cyclohexene oxidation, and it was used to evaluate the transformation from gas phase to particle phase. Particle phase chemical composition was studied by means of Fourier transform infrared (FTIR) spectrometer (Nicolet iS10, Thermos Fisher, USA). The aerosols were sampled through a Dekati low pressure impactor (DLPI, DeKati Ltd, Finland). The impactor was connected to a pump working at a flow rate of 10 L min^{-1} while sampling a total volume of 300 L of gas for each experimental run. Aerosols, from 108 to 650 nm diameter, were collected on an ungreased zinc selenide (ZnSe) disk (25 mm in diameter) for FTIR measurements.

The characteristic bands of inorganic and organic sulfates overlap in the IR spectrum. In order to distinguish between the inorganic and organic sulfates, ion chromatograph (IC, Dionex ICS-900, Thermo Fisher, USA) was used to analyze the inorganic sulfate anion (SO$_4^{2-}$) in SOA. For the IC analysis, the limit of detection was 0.2 mg mL^{-1}. SOA collected on ZnSe disks was firstly dissolved in high purity water (7 mL) and then measured by IC for SO$_4^{2-}$ concentrations. The anions were analyzed with a Dionex IonPac AS14A analytical column and an anion self-regenerating suppressor Dionex ASRS was used as eluent. The flow rate was 1.0 mL min^{-1} with a mixture of 8.0 mmol L^{-1} Na$_2$CO$_3$ and 1.0 mmol L^{-1} NaHCO$_3$ for anions analyses. The suppressing current was 50 mA.

Chemical characterization of aerosols from photooxidation of cyclohexene was performed using an electrospray ionization high-resolution quadrupole mass spectrometer (ESI-HR-MS, Thermo Fisher, USA) operated in negative (-) ion mode, which was calibrated using the manufacturer's calibration standards mixture allowing for mass accuracies <5 ppm in external calibration mode. The ionization voltage was 4.2 kV and the capillary temperature was set at 300 °C. N$_2$ was used as both

the sheath gas (70 U) and auxiliary gas (30 U). SOA was collected on the aluminium foil using the same method as FTIR analysis and then extracted with 1 mL of acetonitrile. The aluminium foil was used due to its ease to handle and its non-reactivity with the sample. A total volume of 300 L was sampled at a flow rate of 10 L min^{-1}. A volume of 5 μL of the extraction and a direct injection were used for the measurement. Xcalibur 2.2 software (Thermo Fisher, USA) was used for the calculation of chemical formula from the accurate measurement of m/z values.

2.4 Chemicals

The chemicals used and their stated purities were as follows: cyclohexene (99%) was obtained from Aldrich and used without further purification. A zero air generator (Model 111, Thermo Scientific, USA) was used to generate clean air. The zero air has no detectable non-methane hydrocarbons (NMHC < 1 ppb), NOx (< 1 ppb), low O_3 concentration (< 3 ppb), and low particle numbers (< 5 cm^{-3}), and relative humidity (RH) below 10%. Ozone was produced from O_2 via electrical discharge using a dynamic gas calibrator (Model 146i, Thermo Scientific, USA). NO_2 (510 ppm), NO (50 ppm) and SO_2 (25 ppm) with ultra-pure N_2 (99.999%) as background gas was purchased from Beijing Huangyuan Gas Co., Ltd., China.

3 Results and discussion

3.1 Effect of SO_2 on SOA number concentrations

The particle number concentrations at the maximum SOA yield for the cyclohexene/NOx/SO_2 system with different initial SO_2 concentrations are shown in Figure 1. The cooperation of the maximum number concentration and the particle number concentrations at the maximum SOA yield is shown in Figure S2. After the black light lamps were turned on, the SOA number concentrations increased rapidly to reach the maximum within 0.5 h in each experiment. Subsequently, the particle number concentrations gradually decreased accompanied by the growth of particle size by coagulation. The SOA mass concentration kept increasing until its maximum was reached (after ~2 h). Both types of particle number concentrations had similar trends against initial SO_2 concentrations. In general, maximum particle number concentrations were three times higher than the particle number concentrations at the maximum SOA yield. In the remainder of this paper, in order to better elaborate the effect of SO_2 on the formation of particles, the particle number concentration refers to the particle number concentrations at the maximum SOA yield.

The particle number concentration increased with initial SO_2 concentration, and this increase could be divided into two stages: increasing stage and stable stage. In the increasing stage, with the initial SO_2 concentration increasing from 0 ppb to 30 ppb, the particle number concentration grew significantly under low initial SO_2 concentration (<5 ppb), then the growth rate reduced gradually. In the stable stage, when the SO_2 concentrations were varied systematically between 30 and 105 ppb, particle number concentrations were practically maintained steady, and there was no further obvious growth as shown in Figure 1. For experiments with high initial SO_2 concentrations, the particle number concentrations were 10 times higher than those without SO_2, indicating enhanced new particle formation (NPF) when adding SO_2. It is evident from Figure 1 that even

Nucleation is a fundamental step in the atmospheric new particle formation. Nucleation of particles in the atmosphere has been observed to be strongly dependent on the abundance of H$_2$SO$_4$ (Sihto et al., 2006; Xiao et al., 2015). Normally, SO$_2$ was deemed to be oxidized by OH radicals to form H$_2$SO$_4$ through homogeneous reactions in gas phase (Calvert et al., 1978), or by H$_2$O$_2$ and O$_3$ through in-cloud processes in aqueous phase (Lelieveld and Heintzenberg, 1992). The aqueous phase formation of H$_2$SO$_4$ is negligible in this study (RH<10%). As the precursor of H$_2$SO$_4$, SO$_2$ at high concentrations would lead to more H$_2$SO$_4$ formation, and thereby increase the nucleation rates and total particle number concentrations (Sipilä et al., 2010). Because of the similar initial conditions for each experiment except SO$_2$, the amount of OH radicals produced was assumed to be almost equal. In the presence of high concentrations of SO$_2$, new particle formation was not enhanced. This feature may indicate that no more sulfates were formed when SO$_2$ was in large excess (>30 ppb) and the OH radicals were insufficient. The quantity of OH radicals is the main restraint on H$_2$SO$_4$ formation at high initial SO$_2$ concentrations, which could not lead to more H$_2$SO$_4$ formation in the present study. Therefore, the particle number concentration was maintained steady, and it was independent of the SO$_2$ concentrations in the second stage.

Besides, the mean diameter of particles increased with photooxidation reaction time, which suggests that not many new particles were generated after a burst increase at the initial stage of SOA formation. Once new particles are formed, there is a competition between growth of existing particles by uptake of the precursors and formation of new particles. Our result agrees with previous studies that there was no obvious increase in aerosol number concentration when additional VOCs were injected, but a significant increase in SOA mass concentration (Presto et al., 2005a). New particles were formed by vapor condensation onto existing aerosol particles. If there was enough seed particle surface area, observation of new particles formation would not be expected.

3.2 Effect of SO$_2$ on SOA yields

SOA yield (Y) is defined as Y=ΔM_0/ΔHC, where ΔM_0 is the produced organic aerosol mass concentration (μg m^{-3}), and ΔHC is the mass concentration of reacted cyclohexene (μg m^{-3}). The SOA yields of cyclohexene at different SO$_2$ concentration as determined by SMPS are shown in Figure 2. The numerical values of the aerosol mass concentration and SOA yields at different conditions are shown in Table 1.

The SOA yields in the absence of SO$_2$ were in the range of 2.7-3.4%, which were an order of magnitude lower than those reported in previous studies (Warren et al., 2009; Keywood et al., 2004; Kalberer et al., 2000). There are three possible explanations to this phenomenon. (1) SOA formation is closely related to the oxidation capacity in the photooxidation experiments and, therefore, is affected by the ratio of [VOC]$_0$/[NOx]$_0$ (Pandis et al., 1991). Experiments performed with different SO$_2$ concentrations indicate that the SOA formation is partly controlled by the ability of the system to oxidize cyclohexene and contribute to the particle mass. As indicated in Figure S3 of the Supplementary material, even at 0 ppb of

SO$_2$, the mass concentration of SOA quickly reaches its maximum. Experiments with higher NOx levels have been proved to get considerably lower SOA yield than those with lower NOx levels at the same VOCs concentration (Song et al., 2005). The reactions of organo-peroxy radicals (RO$_2$) with NO and NO$_2$ instead of peroxy radicals (RO$_2$ or HO$_2$) under high NOx conditions resulted in the formation of volatile organic products and a decreased SOA yield (Lane et al., 2008). It was reported that SOA yield was constant for [VOC]$_0$/[NOx]$_0$>15, but decreased considerably (by a factor of more than 4) as [VOC]$_0$/[NOx]$_0$ decreased (Presto et al., 2005b). In our study, the [VOC]$_0$/[NOx]$_0$ ratio was maintained at about 4.4 to 6.9. Recently, the NOx dependence of SOA formation from photooxidation of β-pinene was comprehensively investigated (Sarrafzadeh et al., 2016), and it was shown that the NOx-induced OH concentration was the major factor influencing the SOA yield. The impacts of NOx on SOA formation were only moderate if the impact of NOx on OH concentration was eliminated. OH concentration in our study was relatively insufficient, which was the main limiting factor for SOA formation. (2) UV light is another factor influencing the SOA yield. SOA yields between dark and UV-illuminated conditions were reported to be different (Presto et al., 2005a). Exposure to UV light could reduce SOA yield by 20-40%, while more volatile products were formed (Griffin et al., 1999). (3) The temperature may have a pronounced influence on SOA yield (Qi et al., 2010; Emanuelsson et al., 2013). At low temperatures, semi-volatile organic compounds would favor the condensation of gas phase species and a higher SOA yield could be expected. Raising the chamber temperature by 10 K should cause a decrease of 10% in aerosol yield (Pathak et al., 2007). SOA yields reported in the present study were obtained at a higher temperature, (307±2 K) than 298 K used in most previous studies. On the basis of the discussion above, the SOA yield from cyclohexene in our study was lower than observed in the previous studies.

SOA yields for the cyclohexene/NOx/SO$_2$ system were measured for initial SO$_2$ mixing ratios of 0-105 ppb. Due to the error associated with the SO$_2$ concentrations measurement, with stronger impact on low values than on higher values, several experiments were performed at SO$_2$ concentrations below 40 ppb. The experimental results showed a clear decrease at first and then an increase in the SOA yield with increasing SO$_2$ concentrations (Figure 2). When SO$_2$ concentrations increased from 0 to 40.8 ppb, there was a remarkable decrease in SOA yield, dropping by about half with the increase of SO$_2$ concentration. For SO$_2$ concentrations higher than 40.8 ppb, SOA yield increased with increasing SO$_2$ concentration. The highest SOA yield was found to be 3.5%, and was at 104.7 ppb SO$_2$ concentration. The lowest SOA yield of cyclohexene photooxidation was obtained at an initial SO$_2$ concentration of 40 ppb. Although the SOA yield increased gradually with the initial SO$_2$ concentration at concentrations higher than 40 ppb, a higher SOA yield than that in the absence of SO$_2$ could not be obtained when the initial SO$_2$ concentration was lower than 85 ppb.

SOA formation was enhanced by the presence of SO$_2$ (Jang et al., 2002), which has been previously attributed to acid-catalyzed heterogeneous reactions and produced an increase of the total organic aerosol mass (Xu et al., 2014). Even small amounts of acid are capable of catalyzing heterogeneous reactions. Both NO and NO$_2$ were used as NOx for the repeated experiments in our study. Although the photooxidation reaction could not happen in the case of NO until it was oxidized to NO$_2$, which means that both NO- and NO$_2$-initiated photooxidation reactions were actually triggered by NO$_2$, the chemistry of SOA formation from both processes is similar. Despite the time of occurrence of the maximum SOA concentration for the

experiment with NO_2 was half an hour earlier than that for the experiment with NO, the results of SOA yield were similar. However, there were some undiscovered processes in the cyclohexene/NOx/SO_2 system that offset potential multifold increases in the SOA yield by acid-catalyzed heterogeneous reactions. The competitive reaction between SO_2 and VOCs might be the reason for the decrease of the SOA yield. SO_2 could be oxidized by OH radicals to form H_2SO_4 (Somnitz, 2004).

Due to the presence of O_3 in our system, the formation of intermediates and their reactions with SO_2 could be expected (Criegee, 1975). However, the importance of these reactions can be kinetically limited. The reaction of cyclohexene with ozone has a rate constant of 8.1×10^{-17} cm^3 molecule^{-1} s^{-1} (Stewart et al., 2013), considerably slower than e.g., its reaction with OH, which has a rate constant of 6.4×10^{-11} cm^3 molecule^{-1} s^{-1} (Aschmann et al., 2012). In addition to the kinetic limitation of the cyclohexene reaction with O_3, the typical concentration of O_3 in our chamber was 200 ppb and hence the importance of cyclohexene reaction with O_3 was expected to be less significant than that of its reaction with OH under any relevant SO_2 conditions. The competitive reaction resulted in a decrease of the concentration of OH radicals, which was one of the main oxidizers for the photooxidation in the chamber. As mentioned above, the photooxidation in this study was at high-NOx conditions and the OH was the main limiting factor for SOA formation because of its relatively low concentration. The change of cyclohexene concentration with time at different initial SO_2 concentrations is shown in Figure S4, wherefrom it can be seen that the reacted cyclohexene concentration at 0 ppb initial SO_2 concentration was slightly higher than that at 90 ppb. The consuming rate of cyclohexene was higher without SO_2 in the chamber, which means that if there was a competition reaction, its effect was very limited. Moreover, in real atmospheric situations where O_3 is found in much higher proportion than OH, cyclohexene would mainly react with O_3 to produce Criegee intermediates, which are good SO_2 oxidizers, and significantly less SOA than in the chamber will be formed. At lower OH radical concentration condition caused by the reaction between SO_2 and OH radical, the formation of SOA was inhibited. It was also found that during the Investigation of Sulfur Chemistry in the Antarctic Troposphere, the OH tends to increase when the influx of SO_2 from above decreases (Mauldin et al., 2004), which means that there is a negative correlation between OH and SO_2 in real atmosphere. Accordingly, SOA yield showed descending trend with the increase of SO_2 concentration when the initial SO_2 concentration was lower than 40 ppb.

When the initial SO_2 concentration was greater than 40 ppb, the acid-catalyzed heterogeneous formation of SOA became more significant (Figure 2). The lowest SOA yield was obtained at 40 ppb initial SO_2 concentration. At this concentration, there was a balance between the inhibition of SOA formation by competitive reactions and the promotion by acid-catalyzed reactions. The same SOA yield was obtained in the absence of SO_2 and at 85 ppb initial SO_2 concentration. The competitive reaction plays an important role on SOA formation, and it should be taken into account in SOA simulation models or air quality models for more accurate prediction. The formation of low volatile organics (e.g. organosulfates) by photooxidation in the presence of SO_2 might be another reason for the increase of the SOA yield.

3.3 Organosulfates formation

When SO_2 was added into the chamber, the acidic aerosol particles were formed by photooxidation of SO_2 in a reaction initiated by OH. The changes in the amounts of SO_4^{2-} in particle phase and the consumption of SO_2 (ΔSO_2) with different initial SO_2 concentrations are shown in Figure 3. The amounts of SO_4^{2-} grew rapidly at low concentration of SO_2, but the relative growth rate became steady in the range of 20-60 ppb initial SO_2 concentrations. It was demonstrated that acid-catalyzed processes could take place when there is a small amount of acid catalyst (5 μg m^{-3}) (Czoschke et al., 2003). In our chamber, the concentration of sulfuric acid was greater than 5 μg m^{-3} when the initial SO_2 concentration was greater than 40 ppb. This indicates that acid-catalyzed reactions were evident in our experiment. However, both the amount and the growth rate of ΔSO_2 increased with initial SO_2 concentrations. Figure 3 shows that the changes with initial SO_2 concentrations were not uniform between the SO_4^{2-} concentration and ΔSO_2, which indicates that besides SO_4^{2-}, other products were formed from the reaction of SO_2.

Typical IR spectra of aerosols from the cyclohexene/NOx/SO_2 system under different SO_2 concentrations are presented in Figure 4. Based on the peak positions in the IR spectra, the functional groups represented by each peak are summarized as follows: the broadband at 3100 to 3300 cm^{-1} is assigned to the O–H stretching of hydroxyl and carboxyl groups (Coury and Dillner, 2008). The peak at 1717 cm^{-1} represents the C=O stretching of aldehydes, ketones, and carboxylic acids. The peaks at 1622 and 1278 cm^{-1} show good correlation and both are assigned to the $-ONO_2$ stretching (Liu et al., 2012; Jia and Xu, 2014). The characteristic absorption band at 1500-1350 cm^{-1} is the C–O stretching and O–H bending of COOH group (Ofner et al., 2011). The absorption peak of sulfate exists in the range of 1200-1000 cm^{-1} (Wu et al., 2013). The band at 1100 cm^{-1} in the IR spectra can be attributed to the sulfate group in organic compounds and sulfate. It has been confirmed that the S=O absorption band in organic sulfate monoesters appears around 1040-1070 cm^{-1} (Chihara, 1958). Although, more studies on bands assignments in organosulfates are not currently available from the literature for further comparison, the 1100 cm^{-1} band from the current FTIR study can reasonably be assigned to S=O in the sulfate group.

The intensities of most absorption bands, such as O-H at 3100-3300 cm^{-1}, C=O at 1717 cm^{-1}, $-ONO_2$ at 1622 and 1278 cm^{-1}, and C-H at 2930 cm^{-1}, have similar trends with the change of SOA yield for initial SO_2 concentrations between 11 and 105 ppb. However, the band of sulfate at 1100 cm^{-1} in IR spectra increases with the rise of initial SO_2 concentration rather than the SOA yield, which suggests the formation of sulfate group in organic compounds and sulfate product from SO_2 photooxidation since, only the relative difference in the intensities of FTIR peaks were studied here. The relative intensity of the band at 1100 cm^{-1} increased by 1.8 times when the initial SO_2 concentration rose from 0 to 44 ppb, while the band increased by 7.2 times when the initial SO_2 concentration was 105 ppb. The intensity of 1100 cm^{-1} band grew slowly at low SO_2 concentrations due to the decrease in the formation of aerosols. To clearly show the amount of sulfate group and sulfate in aerosols, the intensity of the band at 1100 cm^{-1} and the amount of SO_4^{2-} were compared in the same aerosol mass, as shown in Figure 5. The relative intensity was set to 1 when the initial SO_2 concentration was 44.3 ppb.

With the increase of SO_2 concentration, the amount of SO_4^{2-} in unit mass of aerosols increased first and then decreased, which was in negative correlation with SOA yield. The relative band intensities at 1100 cm^{-1}, which represented the intensity of both SO_4^{2-} and the sulfate group in organic compounds, also increased approximately in a linear form with the increase of initial SO_2 concentration (R^2=0.91). If the 1100 cm^{-1} band originated from SO_4^{2-} only, the change of the band intensity would be consistent with SO_4^{2-} concentration in unit mass of aerosols. Figure 5 shows the inconsistency between the FTIR band at 1100 cm^{-1} and the amount SO_4^{2-} as the initial SO_2 concentration, which implies that the 1100 cm^{-1} band originated not only from SO_4^{2-}, but also from other organosulfur compounds. These include organosulfates, which also have the S=O bond, and might contribute to the 1100 cm^{-1} band in the FTIR spectrum. The gap between the FTIR band at 1100 cm^{-1} and SO_4^{2-} can be attributed to the formation of organosulfates.

The composition of the cyclohexene SOA was examined with HR-MS using negative ion mode ESI and the mass spectrum was recorded at a resolution of 10^5 (Figure 6). The OH addition to the C=C bond produces an alkyl peroxyl (RO_2) radical that can react with NO to yield organonitrates (Perring et al., 2013). Although the formation of organonitrates was highly expected, there was no evidence of the presence of N-containing compounds from the main peaks of Figure 6, indicating that organonitrates would be formed at very low concentrations, if at all. A similar conclusion could be observed from Figure 4, when noticing that the -ONO_2 stretching peaks at 1622 and 1230 cm^{-1} have very low intensities. The presumed low concentrations of organonitrates might be due to the low concentration of NO when SOA was formed. RO_2 radicals also react with NO_2 to form peroxy nitrates (RO_2NO_2) on time scales comparable to $RONO_2$ formation. However, RO_2NO_2 are thermally labile and rapidly dissociate at ambient temperatures (Perring et al., 2013). Organosulfates were identified in the particle phase from the chamber experiments. Accurate mass fittings for measured ions of organosulfates in ESI negative ion mode are given in Table 2. As shown in Figure 6 and Table 2, 10 different organosulfates were successfully detected and identified from cyclohexene SOA. These results not only first prove the formation of organosulfates from cyclohexene photooxidation at high-NOx condition in the presence of SO_2, but also provide evidence and reference for organosulfates identification by FTIR-IC joint technique. A deprotonated molecular ion at m/z=195.03322 ($C_6H_{11}O_5S^-$) had the maximum content (more than 60%) of all the organosulfates detected in our study. Its intensity was 6.5 times higher than that of the second highest abundant organosulfate. The intermediate product of cyclohexene reaction with OH, i.e., $CH(O)CH_2CH_2CH_2CH_2\dot{C}HOH$, has a hydroxyl group, and the organosulfate product (m/z=195.03322) would likely form from the intermediate product, not from end product.

The mass spectra show a great abundance of peaks, detected as deprotonated molecular ions (M−H)$^-$ formed via proton abstraction. Most cyclohexene SOA contained carboxylic acid and/or aldehyde moieties. The products of the reaction of OH radicals with cyclohexene in the presence of NO were investigated and were identified as cyclic 1,2-hydroxynitrates and 1,6-hexanedial (Aschmann et al., 2012). These products could not be detected by ESI-HR-MS in our study. Aldehydes could be oxidized by OH radicals to form carboxyls, which have been intensively identified in previous studies (Cameron et al., 2002; Goldsmith et al., 2012). The 1,6-hexanedial might be further oxidized in the atmospheric photooxidation reactions to form the 1,6-adipic acid ($C_6H_{10}O_4$) and 6-oxohexanoicacid ($C_6H_{10}O_3$), which were both observed in our MS spectra. In addition to

the C_6 compounds observed in this study, a $C_5H_7O_3^-$ ion was detected with higher abundance than the C_6 compounds. Although the formation of this C_5 compound might be due to a carbonyl cleavage from a six-carbon atoms chain, a proper mechanism for its formation could not be determined. A C_4 compound was also detected in this study, likely as a result of a carbonyl cleavage from a C_5 compound. However, there was no evidence of the formation of compounds with less than four carbon atoms.

The ESI-HR-MS spectra of particles formed from two different initial SO_2 concentrations are shown in Figure S5. We found no obvious difference in the composition and response of organosulfates with different initial SO_2 concentrations. The relative intensity of m/z = 97, which corresponds to sulfate, was set to 100% in both ESI-HR-MS spectra. The relative intensities of the organosulfates peaks in both spectra were almost unchanged regardless of the initial SO_2 concentration, indicating that the organosulfates yield was associated with sulfate content. Our result is consistent with the results of Minerath et al. and Hatch et al. who observed an increase in organosulfates yield with increasing sulfate concentration (Minerath and Elrod, 2009; Hatch et al., 2011). These observations demonstrate that particle sulfate content is likely a key parameter influencing organosulfates formation.

4 Conclusion

We report a series of chamber experiments studies on the formation of secondary aerosols from the mixture of cyclohexene and SO_2. The experiments were based on Fourier transform infrared spectrometer, ion chromatography and electrospray ionization high-resolution quadrupole mass spectrometer, and were performed under NOx conditions. Although new particle formation was found to be enhanced with increasing SO_2 concentration, the yield of SOA was not enhanced for all SO_2 concentrations between 0 and 105 ppb. The SOA formation decreased at first and then was enhanced for all SO_2 concentration above 40 ppb.

Both acid-catalysis and competitive OH reactions with cyclohexene and SO_2 were found to have important effects on the SOA formation and hence, should be taken into account in SOA simulation models or air quality models for a better understanding of haze pollution. The formation of organosulfates, an important part of atmospheric organic aerosol components, was first observed from cyclohexene SOA. The formation of organosulfates has a great significance for the particulate matter formation under high SO_2 concentrations in the atmosphere.

Acknowledgments

This work was supported by National Natural Science Foundation of China (91644214, 21577080, 41375129), Shenzhen Science and Technology Research and Development Funds, China (JCYJ20150402105524052), and the "Strategic Priority Research Program (B)" of the Chinese Academy of Sciences (XDB05010104).

References

Adams, J. M., Constable, J. V., Guenther, A. B., and Zimmerman, P.: An estimate of natural volatile organic compound emissions from vegetation since the last glacial maximum, Chemosphere, 3, 73-91, doi: 10.1016/S1465-9972(00)00023-4, 2001.

Aschmann, S. M., Arey, J., and Atkinson, R.: Kinetics and products of the reactions of OH radicals with cyclohexene, 1-methyl-1-cyclohexene, cis-cyclooctene, and cis-cyclodecene, J. Phys. Chem. A, 116, 9507-9515, doi: 10.1021/jp307217m, 2012.

Atkinson, R.: Gas-phase tropospheric chemistry of volatile organic compounds: 1. Alkanes and alkenes, J. Phys. Chem. Ref. Data., 26, 215-290, doi: 10.1063/1.556012, 1997.

Attwood, A., Washenfelder, R., Brock, C., Hu, W., Baumann, K., Campuzano-Jost, P., Day, D., Edgerton, E., Murphy, D., and Palm, B.: Trends in sulfate and organic aerosol mass in the southeast US: Impact on aerosol optical depth and radiative forcing, Geophys. Res. Lett., 41, 7701-7709, doi: 10.1002/2014GL061669, 2014.

Baker, B., Guenther, A., Greenberg, J., Goldstein, A., and Fall, R.: Canopy fluxes of 2-methyl-3-buten-2-ol over a ponderosa pine forest by relaxed eddy accumulation: Field data and model comparison, J. Geophys. Res., 104, 26107-26114, doi: Doi 10.1029/1999jd900749, 1999.

Calvert, J. G., Su, F., Bottenheim, J. W., and Strausz, O. P.: Mechanism of the homogeneous oxidation of sulfur dioxide in the troposphere, Atmos. Environ., 12, 197-226, doi: 10.1016/0004-6981(78)90201-9, 1978.

Cameron, M., Sivakumaran, V., Dillon, T. J., and Crowley, J. N.: Reaction between OH and CH_3CHO. Part 1. Primary product yields of CH_3 (296 K), CH_3CO (296 K), and H (237-296 K), Phys. Chem. Chem. Phys., 4, 3628-3638, doi: 10.1039/b202586h, 2002.

Carlsson, P. T., Dege, J. E., Keunecke, C., Kruger, B. C., Wolf, J. L., and Zeuch, T.: Pressure dependent aerosol formation from the cyclohexene gas-phase ozonolysis in the presence and absence of sulfur dioxide: a new perspective on the stabilisation of the initial clusters, Phys. Chem. Chem. Phys., 14, 11695-11705, doi: 10.1039/c2cp40714k, 2012.

Cheng, N., Zhang, D., Li, Y., Chen, T., Li, J., Dong, X., Sun, R., and Meng, F.: Analysis about spatial and temporal distribution of SO_2 and an ambient SO_2 pollution process in Beijing during 2000-2014, Environ. Sci., 36, 3961-3971, doi: 10.13227/j.hjkx.2015.11.004, 2015.

Chihara, G.: Characteristic infrared absorption band of organic sulfate esters, Chem. Pharm. Bull., 6, 114, doi: 10.1248/cpb.6.114, 1958.

Chin, J. Y., and Batterman, S. A.: VOC composition of current motor vehicle fuels and vapors, and collinearity analyses for receptor modeling, Chemosphere, 86, 951-958, doi: 10.1016/j.chemosphere.2011.11.017, 2012.

Coury, C., and Dillner, A. M.: A method to quantify organic functional groups and inorganic compounds in ambient aerosols using attenuated total reflectance FTIR spectroscopy and multivariate chemometric techniques, Atmos. Environ., 42, 5923-5932, doi: 10.1016/j.atmosenv.2008.03.026, 2008.

Criegee, R.: Mechanism of ozonolysis, Angew. Chem. Int. Edit., 14, 745-752, doi: 10.1002/anie.197507451, 1975.

Czoschke, N. M., Jang, M., and Kamens, R. M.: Effect of acidic seed on biogenic secondary organic aerosol growth, Atmos. Environ., 37, 4287-4299, doi: 10.1016/S1352-2310(03)00511-9, 2003.

Darer, A. I., Cole-Filipiak, N. C., O'Connor, A. E., and Elrod, M. J.: Formation and stability of atmospherically relevant isoprene-derived organosulfates and organonitrates, Environ. Sci. Technol., 45, 1895-1902, doi: 10.1021/es103797z, 2011.

Du, L., Xu, Y. F., Ge, M. F., and Jia, L.: Rate constant for the reaction of ozone with diethyl sulfide, Atmos. Environ., 41, 7434-7439, doi: 10.1016/j.atmosenv.2007.05.041, 2007.

Edney, E., Kleindienst, T., Jaoui, M., Lewandowski, M., Offenberg, J., Wang, W., and Claeys, M.: Formation of 2-methyl tetrols and 2-methylglyceric acid in secondary organic aerosol from laboratory irradiated isoprene/NOx/SO₂/air mixtures and their detection in ambient $PM_{2.5}$ samples collected in the eastern United States, Atmos. Environ., 39, 5281-5289, doi: 10.1016/j.atmosenv.2005.05.031, 2005.

Emanuelsson, E. U., Watne, A. K., Lutz, A., Ljungstrom, E., and Hallquist, M.: Influence of humidity, temperature, and radicals on the formation and thermal properties of secondary organic aerosol (SOA) from ozonolysis of β-pinene, J. Phys. Chem. A, 117, 10346-10358, doi: 10.1021/jp4010218, 2013.

Froyd, K. D., Murphy, S. M., Murphy, D. M., de Gouw, J. A., Eddingsaas, N. C., and Wennberg, P. O.: Contribution of isoprene-derived organosulfates to free tropospheric aerosol mass, Proc. Natl. Acad. Sci. U. S. A., 107, 21360-21365, doi: 10.1073/pnas.1012561107, 2010.

Goldsmith, C. F., Green, W. H., and Klippenstein, S. J.: Role of O_2 + QOOH in low-temperature ignition of propane. 1. Temperature and pressure dependent rate coefficients, J. Phys. Chem. A, 116, 3325-3346, doi: 10.1021/jp210722w, 2012.

Griffin, R. J., Cocker, D. R., Flagan, R. C., and Seinfeld, J. H.: Organic aerosol formation from the oxidation of biogenic hydrocarbons, J. Geophys. Res., 104, 3555-3567, doi: Doi 10.1029/1998jd100049, 1999.

Grosjean, D., Cauwenberghe, K. V., Schmid, J. P., Kelley, P. E., and Pitts, J. N.: Identification of C3-C10 aliphatic dicarboxylic acids in airborne particulate matter, Environ. Sci. Technol., 12, 313-317, doi: 10.1021/es60139a005, 1978.

Hallquist, M., Wenger, J. C., Baltensperger, U., Rudich, Y., Simpson, D., Claeys, M., Dommen, J., Donahue, N. M., George, C., Goldstein, A. H., Hamilton, J. F., Herrmann, H., Hoffmann, T., Iinuma, Y., Jang, M., Jenkin, M. E., Jimenez, J. L., Kiendler-Scharr, A., Maenhaut, W., McFiggans, G., Mentel, T. F., Monod, A., Prevot, A. S. H., Seinfeld, J. H., Surratt, J. D., Szmigielski, R., and Wildt, J.: The formation, properties and impact of secondary organic aerosol: current and emerging issues, Atmos. Chem. Phys., 9, 5155-5236, doi: 10.5194/acpd-9-3555-2009 2009.

Hansen, J. E., and Sato, M.: Trends of measured climate forcing agents, Proc. Natl. Acad. Sci. U. S. A., 98, 14778-14783, doi: 10.1073/pnas.261553698, 2001.

Hatch, L. E., Creamean, J. M., Ault, A. P., Surratt, J. D., Chan, M. N., Seinfeld, J. H., Edgerton, E. S., Su, Y. X., and Prather, K. A.: Measurements of isoprene-derived organosulfates in ambient aerosols by aerosol time-of-flight mass spectrometry-part 1: Single particle atmospheric observations in atlanta, Environ. Sci. Technol., 45, 5105-5111, doi: 10.1021/es103944a, 2011.

Hu, K. S., Darer, A. I., and Elrod, M. J.: Thermodynamics and kinetics of the hydrolysis of atmospherically relevant organonitrates and organosulfates, Atmos. Chem. Phys., 11, 8307-8320, doi: 10.5194/acp-11-8307-2011, 2011.

Jang, M., Czoschke, N. M., Lee, S., and Kamens, R. M.: Heterogeneous atmospheric aerosol production by acid-catalyzed particle-phase reactions, Science, 298, 814-817, doi: 10.1126/science.1075798, 2002.

Jaoui, M., Kleindienst, T. E., Offenberg, J. H., Lewandowski, M., and Lonneman, W. A.: SOA formation from the atmospheric oxidation of 2-methyl-3-buten-2-ol and its implications for $PM_{2.5}$, Atmos. Chem. Phys., 12, 2173-2188, doi: 10.5194/acp-12-2173-2012, 2012.

Jia, L., and Xu, Y. F.: Effects of relative humidity on ozone and secondary organic aerosol formation from the photooxidation of benzene and ethylbenzene, Aerosol. Sci. Tech., 48, 1-12, doi: 10.1080/02786826.2013.847269, 2014.

Jimenez, J. L., Canagaratna, M. R., Donahue, N. M., Prevot, A. S. H., Zhang, Q., Kroll, J. H., Decarlo, P. F., Allan, J. D., Coe, H., and Ng, N. L.: Evolution of organic aerosols in the atmosphere, Science, 326, 1525-1529, doi: 10.1126/science.1180353, 2009.

Kalberer, M., Yu, J., Cocker, D. R., Flagan, R. C., and Seinfeld, J. H.: Aerosol formation in the cyclohexene-ozone system, Environ. Sci. Technol., 34, 4894-4901, doi: 10.1021/es001180f, 2000.

Kanakidou, M., Seinfeld, J. H., Pandis, S. N., Barnes, I., Dentener, F. J., Facchini, M. C., Van Dingenen, R., Ervens, B., Nenes, A., Nielsen, C. J., Swietlicki, E., Putaud, J. P., Balkanski, Y., Fuzzi, S., Horth, J., Moortgat, G. K., Winterhalter, R., Myhre, C. E. L., Tsigaridis, K., Vignati, E., Stephanou, E. G., and Wilson, J.: Organic aerosol and global climate modelling: a review, Atmos. Chem. Phys., 5, 1053-1123, doi: 10.5194/acp-5-1053-2005, 2005.

Kesselmeier, J., Kuhn, U., Rottenberger, S., Biesenthal, T., Wolf, A., Schebeske, G., Andreae, M. O., Ciccioli, P., Brancaleoni, E., Frattoni, M., Oliva, S. T., Botelho, M. L., Silva, C. M. A., and Tavares, T. M.: Concentrations and species composition of atmospheric volatile organic compounds (VOCs) as observed during the wet and dry season in Rondonia (Amazonia), J. Geophys. Res., 107, LBA 20-21–LBA 20-13, doi: 10.1029/2000jd000267, 2002.

Keywood, M. D., Varutbangkul, V., Bahreini, R., Flagan, R. C., and Seinfeld, J. H.: Secondary organic aerosol formation from the ozonolysis of cycloalkenes and related compounds, Environ. Sci. Technol., 38, 4157-4164, doi: 10.1021/es035363o, 2004.

Kristensen, K., and Glasius, M.: Organosulfates and oxidation products from biogenic hydrocarbons in fine aerosols from a forest in North West Europe during spring, Atmos. Environ., 45, 4546-4556, doi: 10.1016/j.atmosenv.2011.05.063, 2011.

Kroll, J. H., and Seinfeld, J. H.: Chemistry of secondary organic aerosol: Formation and evolution of low-volatility organics in the atmosphere, Atmos. Environ., 42, 3593-3624, doi: 10.1016/j.atmosenv.2008.01.003, 2008.

Lane, T. E., Donahue, N. M., and Pandis, S. N.: Effect of NOx on secondary organic aerosol concentrations, Environ. Sci. Technol., 42, 6022-6037, doi: 10.1021/es703225a, 2008.

Lelieveld, J., and Heintzenberg, J.: Sulfate cooling effect on climate through in-cloud oxidation of anthropogenic SO_2, Science, 258, 117-120, doi: 10.1126/science.258.5079.117, 1992.

Lin, Y. H., Zhang, Z. F., Docherty, K. S., Zhang, H. F., Budisulistiorini, S. H., Rubitschun, C. L., Shaw, S. L., Knipping, E. M., Edgerton, E. S., Kleindienst, T. E., Gold, A., and Surratt, J. D.: Isoprene epoxydiols as precursors to secondary organic aerosol formation: acid-catalyzed reactive uptake studies with authentic compounds, Environ. Sci. Technol., 46, 250-258, doi: 10.1021/es202554c, 2012.

Liu, S., Shilling, J. E., Song, C., Hiranuma, N., Zaveri, R. A., and Russell, L. M.: Hydrolysis of organonitrate functional groups in aerosol particles, Aerosol. Sci. Tech., 46, 1359-1369, doi: 10.1080/02786826.2012.716175, 2012.

Liu, T., Wang, X., Hu, Q., Deng, W., Zhang, Y., Ding, X., Fu, X., Bernard, F., Zhang, Z., and Lü, S.: Formation of secondary aerosols from gasoline vehicle exhausts when mixing with SO_2, Atmos. Chem. Phys., 16, 675-689, doi: 10.5194/acp-16-675-2016, 2016.

Lonsdale, C. R., Stevens, R. G., Brock, C. A., Makar, P. A., Knipping, E. M., and Pierce, J. R.: The effect of coal-fired power-plant SO_2 and NOx control technologies on aerosol nucleation in the source plumes, Atmos. Chem. Phys., 12, 11519-11531, doi: 10.5194/acp-12-11519-2012, 2012.

Mael, L. E., Jacobs, M. I., and Elrod, M. J.: Organosulfate and nitrate formation and reactivity from epoxides derived from 2-methyl-3-buten-2-ol, J. Phys. Chem. A, 119, 4464-4472, doi: 10.1021/jp510033s, 2015.

Mauldin, R., Kosciuch, E., Henry, B., Eisele, F., Shetter, R., Lefer, B., Chen, G., Davis, D., Huey, G., and Tanner, D.: Measurements of OH, HO_2+RO_2, H_2SO_4, and MSA at the south pole during ISCAT 2000, Atmos. Environ., 38, 5423-5437, doi: 10.1016/j.atmosenv.2004.06.031 2004.

McFiggans, G., Artaxo, P., Baltensperger, U., Coe, H., Facchini, M. C., Feingold, G., Fuzzi, S., Gysel, M., Laaksonen, A., Lohmann, U., Mentel, T. F., Murphy, D. M., O'Dowd, C. D., Snider, J. R., and Weingartner, E.: The effect of physical and chemical aerosol properties on warm cloud droplet activation, Atmos. Chem. Phys., 6, 2593-2649, doi: 10.5194/acp-6-2593-2006, 2006.

Minerath, E. C., and Elrod, M. J.: Assessing the potential for diol and hydroxy sulfate ester formation from the reaction of epoxides in tropospheric aerosols, Environ. Sci. Technol., 43, 1386-1392, 2009.

Nah, T., Sanchez, J., Boyd, C. M., and Ng, N. L.: Photochemical aging of alpha-pinene and beta-pinene secondary organic aerosol formed from nitrate radical oxidation, Environ. Sci. Technol., 50, 222-231, doi: 10.1021/acs.est.5b04594, 2016.

Ofner, J., Kruger, H. U., Grothe, H., Schmitt-Kopplin, P., Whitmore, K., and Zetzsch, C.: Physico-chemical characterization of SOA derived from catechol and guaiacol-a model substance for the aromatic fraction of atmospheric HULIS, Atmos. Chem. Phys., 11, 1-15, doi: 10.5194/acp-11-1-2011, 2011.

Pandis, S. N., Paulson, S. E., Seinfeld, J. H., and Flagan, R. C.: Aerosol formation in the photooxidation of isoprene and β-pinene, Atmos. Environ., 25, 997-1008, doi: 10.1016/0960-1686(91)90141-S, 1991.

Passananti, M., Kong, L., Shang, J., Dupart, Y., Perrier, S., Chen, J., Donaldson, D. J., and George, C.: Organosulfate formation through the heterogeneous reaction of sulfur dioxide with unsaturated fatty acids and long-chain alkenes, Angew. Chem.-Int. Edit., 55, 10336-10339, doi: 10.1002/anie.201605266, 2016.

Pathak, R. K., Stanier, C. O., Donahue, N. M., and Pandis, S. N.: Ozonolysis of alpha-pinene at atmospherically relevant concentrations: Temperature dependence of aerosol mass fractions (yields), J. Geophys. Res., 112, doi: 10.1029/2006jd007436, 2007.

Paulson, S. E., and Orlando, J. J.: The reactions of ozone with alkenes: An important source of HOx in the boundary layer, Geophys. Res. Lett., 23, 3727-3730, doi: 10.1029/96GL03477, 1996.

Paulson, S. E., Chung, M. Y., and Hasson, A. S.: OH radical formation from the gas-phase reaction of ozone with terminal alkenes and the relationship between structure and mechanism, J. Phys. Chem. A, 103, 8125-8138, doi: Doi 10.1021/Jp991995e, 1999.

Perring, A. E., Pusede, S. E., and Cohen, R. C.: An observational perspective on the atmospheric impacts of alkyl and multifunctional nitrates on ozone and secondary organic aerosol, Chem. Rev., 113, 5848-5870, doi: 10.1021/cr300520x, 2013.

Pokhrel, A., Kawamura, K., Ono, K., Seki, O., Fu, P. Q., Matoba, S., and Shiraiwa, T.: Ice core records of monoterpene- and isoprene-SOA tracers from Aurora Peak in Alaska since 1660s: Implication for climate change variability in the North Pacific Rim, Atmos. Environ., 130, 105-112, doi: 10.1016/j.atmosenv.2015.09.063, 2016.

Pope III, C. A., and Dockery, D. W.: Health effects of fine particulate air pollution: lines that connect, J. Air Waste Manage. Assoc., 56, 709-742, doi: 10.1080/10473289.2006.10464485, 2006.

Presto, A. A., Hartz, K. E., and Donahue, N. M.: Secondary organic aerosol production from terpene ozonolysis. 1. Effect of UV radiation, Environ. Sci. Technol., 39, 7036-7045, doi: 10.1021/es050174m, 2005a.

Presto, A. A., Hartz, K. E., and Donahue, N. M.: Secondary organic aerosol production from terpene ozonolysis. 2. Effect of NOx concentration, Environ. Sci. Technol., 39, 7046-7054, doi: 10.1021/es050400s, 2005b.

Qi, L., Nakao, S., Tang, P., and Cocker, D. R.: Temperature effect on physical and chemical properties of secondary organic aerosol from m-xylene photooxidation, Atmos. Chem. Phys., 10, 3847-3854, doi: 10.5194/acp-10-3847-2010, 2010.

Reddy, M. S., and Venkataraman, C.: Inventory of aerosol and sulphur dioxide emissions from India. Part II-biomass combustion, Atmos. Environ., 36, 699-712, doi: Doi 10.1016/S1352-2310(01)00464-2, 2002.

Riva, M., Tomaz, S., Cui, T., Lin, Y. H., Perraudin, E., Gold, A., Stone, E. A., Villenave, E., and Surratt, J. D.: Evidence for an unrecognized secondary anthropogenic source of organosulfates and sulfonates: gas-phase oxidation of polycyclic aromatic hydrocarbons in the presence of sulfate aerosol, Environ. Sci. Technol., 49, 6654-6664, doi: 10.1021/acs.est.5b00836, 2015.

Riva, M., Budisulistiorini, S. H., Chen, Y., Zhang, Z., D'Ambro, E. L., Zhang, X., Gold, A., Turpin, B. J., Thornton, J. A., Canagaratna, M. R., and Surratt, J. D.: Chemical characterization of secondary organic aerosol from oxidation of isoprene hydroxyhydroperoxides, Environ. Sci. Technol., 50, 9889-9899, doi: 10.1021/acs.est.6b02511, 2016.

Romero, F., and Oehme, M.: Organosulfates – A new component of humic-like substances in atmospheric aerosols?, J. Atmos. Chem., 52, 283-294, doi: 10.1007/s10874-005-0594-y, 2005.

Sakamoto, Y., Inomata, S., and Hirokawa, J.: Oligomerization reaction of the Criegee intermediate leads to secondary organic aerosol formation in ethylene ozonolysis, J. Phys. Chem. A, 117, 12912-12921, doi: 10.1021/jp408672m, 2013.

Sarrafzadeh, M., Wildt, J., Pullinen, I., Springer, M., Kleist, E., Tillmann, R., Schmitt, S. H., Wu, C., Mentel, T. F., and Zhao, D.: Impact of NOx and OH on secondary organic aerosol formation from β-pinene photooxidation, Atmos. Chem. Phys., 16, 11237-11248, doi: 10.5194/acp-16-11237-2016, 2016.

Sarwar, G., and Corsi, R.: The effects of ozone/limonene reactions on indoor secondary organic aerosols, Atmos. Environ., 41, 959-973, doi: 10.1016/j.atmosenv.2006.09.032, 2007.

Shalamzari, M. S., Ryabtsova, O., Kahnt, A., Vermeylen, R., Herent, M. F., Quetin-Leclercq, J., Van der Veken, P., Maenhaut, W., and Claeys, M.: Mass spectrometric characterization of organosulfates related to secondary organic aerosol from isoprene, Rapid Commun. Mass Spectrom., 27, 784-794, doi: 10.1002/rcm.6511, 2013.

Sihto, S. L., Kulmala, M., Kerminen, V. M., Dal Maso, M., Petaja, T., Riipinen, I., Korhonen, H., Arnold, F., Janson, R., Boy, M., Laaksonen, A., and Lehtinen, K. E. J.: Atmospheric sulphuric acid and aerosol formation: implications from atmospheric measurements for nucleation and early growth mechanisms, Atmos. Chem. Phys., 6, 4079-4091, doi: 10.5194/acp-6-4079-2006, 2006.

Sipilä, M., Berndt, T., Petaja, T., Brus, D., Vanhanen, J., Stratmann, F., Patokoski, J., Mauldin, R. L., 3rd, Hyvarinen, A. P., Lihavainen, H., and Kulmala, M.: The role of sulfuric acid in atmospheric nucleation, Science, 327, 1243-1246, doi: 10.1126/science.1180315, 2010.

Sipilä, M., Jokinen, T., Berndt, T., Richters, S., Makkonen, R., Donahue, N. M., Mauldin, R. L., III, Kurten, T., Paasonen, P., and Sarnela, N.: Reactivity of stabilized Criegee intermediates (sCI) from isoprene and monoterpene ozonolysis toward SO_2 and organic acids, Atmos. Chem. Phys., 14, 3071-3098, doi: 10.5194/acpd-14-3071-2014, 2013.

Somnitz, H.: Quantum chemical and dynamical characterisation of the reaction $OH+SO_2 \rightleftharpoons HOSO_2$ over an extended range of temperature and pressure, Phys. Chem. Chem. Phys., 6, 3844-3851, doi: 10.1039/b317055a, 2004.

Song, C., Na, K., and Cocker, D. R., 3rd: Impact of the hydrocarbon to NOx ratio on secondary organic aerosol formation, Environ. Sci. Technol., 39, 3143-3149, doi: 10.1021/es0493244, 2005.

Staudt, S., Kundu, S., Lehmler, H. J., He, X., Cui, T., Lin, Y. H., Kristensen, K., Glasius, M., Zhang, X., Weber, R. J., Surratt, J. D., and Stone, E. A.: Aromatic organosulfates in atmospheric aerosols: synthesis, characterization, and abundance, Atmos. Environ., 94, 366-373, doi: 10.1016/j.atmosenv.2014.05.049, 2014.

Stewart, D. J., Almabrok, S. H., Lockhart, J. P., Mohamed, O. M., Nutt, D. R., Pfrang, C., and Marston, G.: The kinetics of the gas-phase reactions of selected monoterpenes and cyclo-alkenes with ozone and the NO_3 radical, Atmos. Environ., 70, 227-235, doi: 10.1016/j.atmosenv.2013.01.036, 2013.

Sun, H., Li, S., Zhang, Y., Jiang, H., Qu, L., Liu, Z., and Liu, S.: Selective hydrogenation of benzene to cydohexene in continuous reaction device with two reaction reactors in serie over Ru-Co-B/ZrO_2 catalysts, Chin. J. Catal., 34, 1482-1488, doi: 10.1016/S1872-2067(12)60637-8, 2013.

Surratt, J. D., Kroll, J. H., Kleindienst, T. E., Edney, E. O., Claeys, M., Sorooshian, A., Ng, N. L., Offenberg, J. H., Lewandowski, M., Jaoui, M., Flagan, R. C., and Seinfeld, J. H.: Evidence for organosulfates in secondary organic aerosol, Environ. Sci. Technol., 41, 517-527, doi: 10.1021/es062081q, 2007.

Surratt, J. D., Gomez-Gonzalez, Y., Chan, A. W., Vermeylen, R., Shahgholi, M., Kleindienst, T. E., Edney, E. O., Offenberg, J. H., Lewandowski, M., Jaoui, M., Maenhaut, W., Claeys, M., Flagan, R. C., and Seinfeld, J. H.: Organosulfate formation in biogenic secondary organic aerosol, J. Phys. Chem. A, 112, 8345-8378, doi: 10.1021/jp802310p, 2008.

Tolocka, M. P., and Turpin, B.: Contribution of organosulfur compounds to organic aerosol mass, Environ. Sci. Technol., 46, 7978-7983, doi: 10.1021/es300651v, 2012.

Wang, X. K., Rossignol, S., Ma, Y., Yao, L., Wang, M. Y., Chen, J. M., George, C., and Wang, L.: Identification of particulate organosulfates in three megacities at the middle and lower reaches of the Yangtze River, Atmos. Chem. Phys., 15, 21415-21448, doi: 10.5194/acpd-15-21415-2015, 2015.

Wang, X. M., Carmichael, G., Chen, D. L., Tang, Y. H., and Wang, T. J.: Impacts of different emission sources on air quality during March 2001 in the Pearl River Delta (PRD) region, Atmos. Environ., 39, 5227-5241, doi: 10.1016/j.atmosenv.2005.04.035, 2005.

Warren, B., Malloy, Q. G. J., Yee, L. D., and Cocker, D. R.: Secondary organic aerosol formation from cyclohexene ozonolysis in the presence of water vapor and dissolved salts, Atmos. Environ., 43, 1789-1795, doi: 10.1016/j.atmosenv.2008.12.026, 2009.

Wu, L. Y., Tong, S. R., Zhou, L., Wang, W. G., and Ge, M. F.: Synergistic Effects between SO_2 and HCOOH on α-Fe_2O_3, J. Phys. Chem. A, 117, 3972-3979, doi: 10.1021/jp400195f, 2013.

Xiao, S., Wang, M. Y., Yao, L., Kulmala, M., Zhou, B., Yang, X., Chen, J. M., Wang, D. F., Fu, Q. Y., Worsnop, D. R., and Wang, L.: Strong atmospheric new particle formation in winter in urban Shanghai, China, Atmos. Chem. Phys., 15, 1769-1781, doi: 10.5194/acp-15-1769-2015, 2015.

Xu, W., Gomez-Hernandez, M., Guo, S., Secrest, J., Marrero-Ortiz, W., Zhang, A. L., and Zhang, R.: Acid-catalyzed reactions of epoxides for atmospheric nanoparticle growth, J. Am. Chem. Soc., 136, 15477-15480, doi: 10.1021/ja508989a, 2014.

Zhang, H., Worton, D. R., Lewandowski, M., Ortega, J., Rubitschun, C. L., Park, J. H., Kristensen, K., Campuzano-Jost, P., Day, D. A., Jimenez, J. L., Jaoui, M., Offenberg, J. H., Kleindienst, T. E., Gilman, J., Kuster, W. C., de Gouw, J., Park, C., Schade, G. W., Frossard, A. A., Russell, L., Kaser, L., Jud, W., Hansel, A., Cappellin, L., Karl, T., Glasius, M., Guenther, A., Goldstein, A. H., Seinfeld, J. H., Gold, A., Kamens, R. M., and Surratt, J. D.: Organosulfates as tracers for secondary organic aerosol (SOA) formation from 2-methyl-3-buten-2-ol (MBO) in the atmosphere, Environ. Sci. Technol., 46, 9437-9446, doi: 10.1021/es301648z, 2012.

Zhang, H., Zhang, Z., Cui, T., Lin, Y. H., Bhathela, N. A., Ortega, J., Worton, D. R., Goldstein, A. H., Guenther, A., Jimenez, J. L., Gold, A., and Surratt, J. D.: Secondary organic aerosol formation via 2-Methyl-3-buten-2-ol photooxidation: evidence of acid-catalyzed reactive uptake of epoxides, Environ. Sci. Technol. Lett., 1, 242-247, doi: 10.1021/ez500055f, 2014.

Zhang, X., Schwantes, R. H., McVay, R. C., Lignell, H., Coggon, M. M., Flagan, R. C., and Seinfeld, J. H.: Vapor wall deposition in Teflon chambers, Atmos. Chem. Phys., 15, 4197-4214, doi: 10.5194/acp-15-4197-2015, 2015.
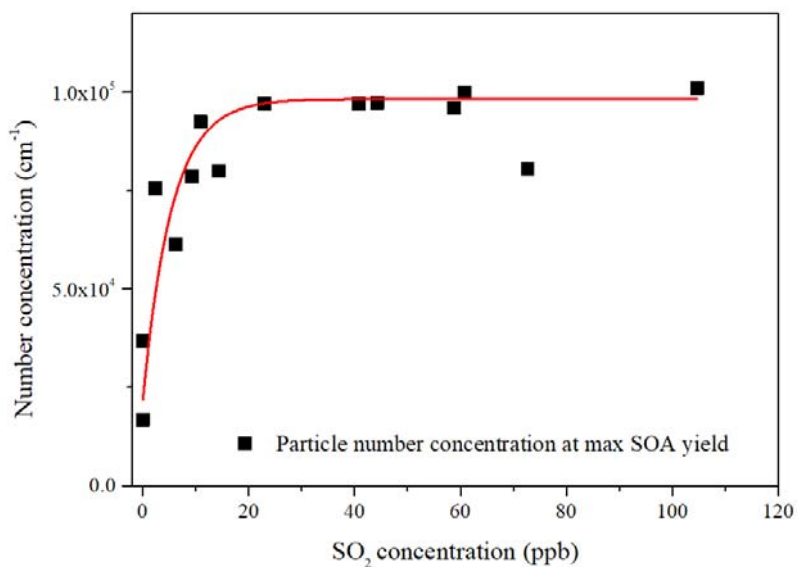
Figure 1: Particle number concentrations of SOA in the photooxidation of the cyclohexene/NOx/SO$_2$ system with different initial SO$_2$ concentrations.
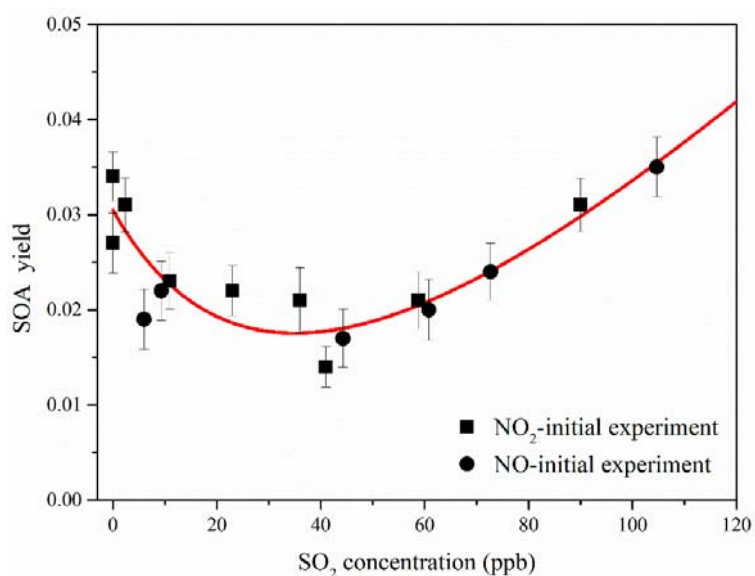
Figure 2: SOA yields of cyclohexene photooxidation in the presence of NOx at different initial SO$_2$ concentrations. Solid line is the least-square fitting to the data. The error bars were determined on the basis of propagation of uncertainties arising in the ΔHC measurements, including GC calibration uncertainties propagation and the variance in the initial cyclohexene measurements.
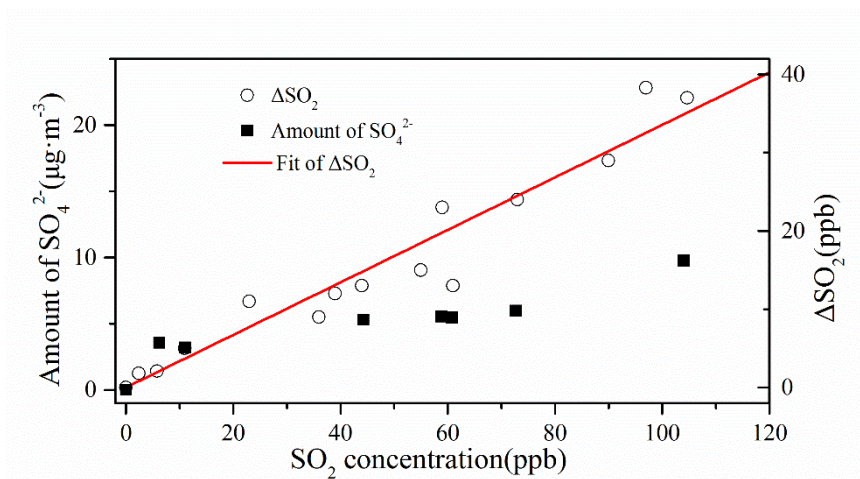
Figure 3: The amount of SO₄²⁻ in aerosols in the chamber, consumption of SO₂ (ΔSO₂) and the ratio of the amount of SO₂ for SO₄²⁻ formation to ΔSO₂ with different initial SO₂ concentrations.
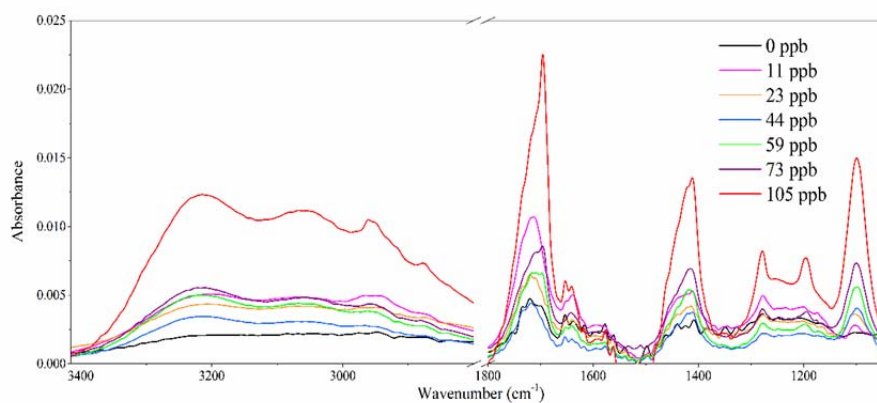
Figure 4: IR spectra of aerosols from the cyclohexene/NOx/SO₂ system under different SO₂ concentrations.
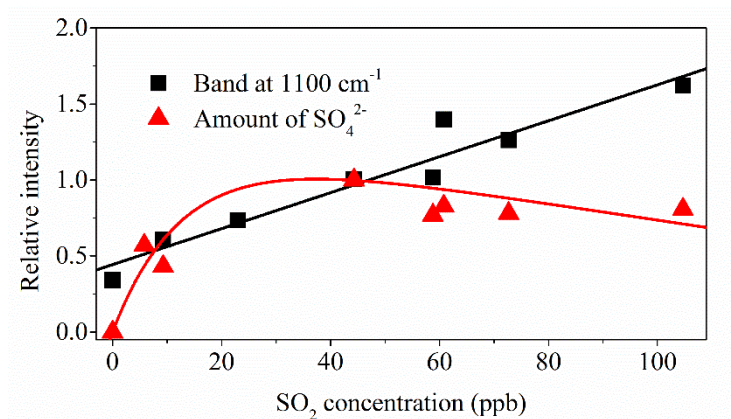
Figure 5: The relative intensity of the FTIR band at 1100 cm^{-1} (square) and the amount of SO$_4^{2-}$ (triangle) normalized to SOA mass. The 1100 cm^{-1} band intensity and the amount of SO$_4^{2-}$ were divided by the formed SOA mass. Subsequently, the results of both FTIR band at 1100 cm^{-1} and the amount of SO$_4^{2-}$ divided by SOA mass were set to 1 when the initial SO$_2$ concentration was 44.3 ppb.
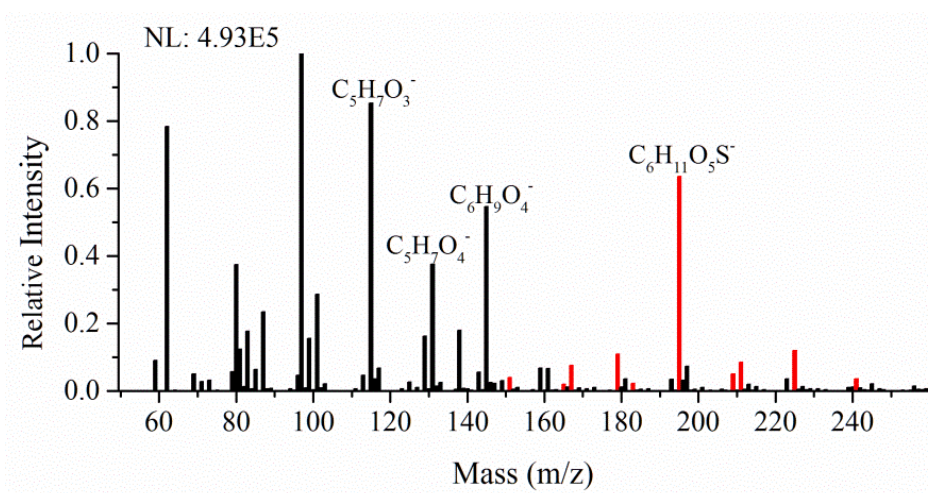
Figure 6: Negative ion mode ESI mass spectrum of SOA generated from the photooxidation of cyclohexene in the presence of SO$_2$. Red peaks correspond to organic compounds containing the sulfate group. The mass resolution is 10^5.

Table 1 Experimental conditions for the photooxidation of cyclohexene/NOx/SO$_2$ system. All experiments were performed under dry conditions (relative humidity < 10 %). ΔM$_0$ is the produced organic aerosol mass concentration and Y is the SOA yield.

Exp.	T (K)	SO$_2$ (ppb)	cyclohexene (ppb)	NOx (ppb)	cyclohexene/NOx	ΔM$_0$ ($\mu g\ m^{-3}$)	Y (%)
1[b]	308	0.0	596	122.0	4.9	57.0	2.66
2[b]	305	0.0	651	93.7	6.9	79.7	3.40
3[b]	309	2.4	553	95.7	5.8	62.6	3.15
4[a]	307	5.8	612	92.7	6.6	41.0	1.87
5[a]	309	9.3	599	93.5	6.4	48.1	2.23
6[b]	309	11.0	574	94.7	6.1	47.1	2.28
7[b]	309	23.0	514	90.5	5.7	42.6	2.30
8[b]	305	36.6	665	99.7	6.7	96.3	2.01
9[b]	308	40.8	472	91.4	5.2	22.6	1.33
10[a]	308	44.3	592	98.6	6.0	35.3	1.66
11[b]	305	55.0	497	113.0	4.4	77.3	2.16
12[b]	308	58.8	577	96.7	6.0	44.3	2.13
13[a]	309	60.8	626	102.0	6.1	43.9	1.95
14[a]	308	72.7	581	98.4	5.9	49.2	2.35
15[b]	306	90.0	543	99.6	5.4	102.0	2.62
16[a]	309	104.7	608	93.7	6.5	77.1	3.52
17[bc]	305	236.0	1048	198.0	5.3	-	-
18[bc]	306	93.7	1235	215	5.7	-	-

[a]: the experiment was initiated by NO.

[b]: the experiment was initiated by NO$_2$.

[c]: the formed particles were detected by ESI-HR-MS.

Table 2. Accurate mass fittings for main products and measured organosulfates ions in ESI negative ion mode from cyclohexene photooxidation in the presence of SO$_2$ under high-NOx conditions

Measured [a] m/z	Ion	Proposed Ion Formula	Delta [b] (ppm)	RDB [c]
115.03942		$C_5H_7O_3^-$	-5.628	2
145.05019		$C_6H_9O_4^-$	-3.048	2
131.03444		$C_5H_7O_4^-$	-4.136	2
101.06006	(M−H)$^-$	$C_5H_9O_2^-$	-7.351	1
87.04433		$C_4H_7O_2^-$	-9.453	1
129.05515		$C_6H_9O_3^-$	-4.397	2
99.04439		$C_5H_7O_2^-$	-7.702	2
Organosulfates				
195.03322		$C_6H_{11}O_5S^-$	-0.243	1
225.00771		$C_6H_9O_7S^-$	1.171	2
179.00181		$C_5H_7O_5S^-$	-0.0879	2
211.02828		$C_6H_{11}O_6S^-$	0.464	1
167.00167	(M−H)$^-$	$C_4H_7O_5S^-$	-1.780	1
209.01257		$C_6H_9O_6S^-$	0.182	2
151.00658		$C_4H_7O_4S^-$	-3.130	1
241.00278		$C_6H_9O_8S^-$	1.738	2
182.99667		$C_4H_7O_6S^-$	-1.158	1
164.98594		$C_4H_5O_5S^-$	-2.287	2

[a] Sort by abundance intensity.

[b] Delta: label the peak with the difference between the theoretical and measured m/z.

[c] RDB: ring and double bond equivalent.